Polymer Testing 28 (2009) 324–330

Contents lists available at ScienceDirect

Polymer Testing

journal homepage: www.elsevier.com/locate/polytest

Material Behaviour

On the nonlinear evolution of the Poisson's ratio under quasi-static loading for a carbon fabric-reinforced thermoplastic. Part II: Analytical explanation

I. De Baere*, W. Van Paepegem, J. Degrieck

Department of Materials Science and Engineering, Faculty of Engineering, Ghent University, Sint-Pietersnieuwstraat 41, B-9000 Gent, Belgium

ARTICLE INFO

Article history:
Received 10 December 2008
Accepted 21 January 2009

Keywords:
Composite
Carbon fibre
Polyphenylene sulphide
Poisson's ratio

ABSTRACT

When observing or describing the damage state in a composite material, often only Young's modulus or residual deformation are considered. Generally, however, the Poisson's ratio is more sensitive to damage than those properties. Rather than observing the Poisson's ratio as function of crack density, the evolution of the Poisson's ratio as function of the longitudinal strain was studied in part I of this research, where a peculiar shape of the evolution was observed and proven to be entirely due to the material itself, rather than the sensors used for the strain measurement.

In this article, a theoretical explanation for the peculiar evolution of the Poisson's ratio as function of the longitudinal strain is presented. Based on this explanation, extra experiments were conducted for validation purposes.

The material used for this study is a carbon fabric-reinforced PPS.

1. Introduction

As was already mentioned in part I of this study [1], generally, Poisson's ratio is more sensitive to damage than Young's modulus or residual (or permanent) deformation [2–6]. The decrease in Poisson's ratio is usually explained by the occurrence of transverse cracking, causing elongation in the longitudinal direction. These transverse cracks originate from failure in the transverse plies, but the cracks remain open, causing the elongation, because of the release of thermal (or residual) stresses resulting from the curing or production process [7–11].

For the carbon fabric-reinforced polyphenylene sulphide considered in this paper, these thermal or residual stresses will be relatively high because of the following factors: (i) the reinforcement is carbon, which has a negative thermal expansion coefficient in the fibre direction and, therefore, is more likely to shrink at the elevated temperature during hot pressing; (ii) the polyphenylene sulphide is a semi-crystalline polymer and (iii) the temperatures in compression moulding for thermoplastics are higher compared to the curing temperatures for thermosets.

The difference in thermal stresses between the amorphous and the semi-crystalline matrices is due to the following: the amorphous matrix is in a visco-elastic state between the processing temperature and the glass transition temperature (T_G), meaning that possible stress build-up due to thermal shrinkage can still be relaxed. Once T_G is reached, the amorphous polymer becomes glassy (thermo-elastic state) and residual stresses are formed.

For the semi-crystalline matrix, the stress build-up can only be relaxed until the crystallisation temperature, since then crystals are formed which can carry load. As such, it is more difficult to relax the stress build-up. The residual thermal stresses are the consequence of a larger temperature difference, since the crystallisation temperature is higher than the glass transition temperature and, therefore,

* Corresponding author. Tel.: +32 9 264 32 55; fax: +32 9 264 35 87.
E-mail address: ives.debaere@ugent.be (I. De Baere).

0142-9418/$ – see front matter © 2009 Elsevier Ltd. All rights reserved.
doi:10.1016/j.polymertesting.2009.01.006

the stresses are a lot higher. In fact, they are known to cause micro-cracking simply by cooling the plate to room temperature [6,9].

In the first part of this study [1], the relation between the Poisson's ratio and the longitudinal strain was studied and a peculiar behaviour was found. Therefore, it was investigated whether this behaviour was due to the transverse strain sensors used and, eventually, it was concluded that the shape of the ν_{12}–ε_{xx} curve was entirely due to the material. Therefore, this paper tries to give and validate a theoretical explanation for this behaviour.

In the next section, the material used is discussed. This is followed by a short overview of the experiments, after which a discussion is given. Finally, some conclusions are drawn.

2. Materials and methods

2.1. Composite material

The material under study was a carbon fibre-reinforced polyphenylene sulphide (PPS), called CETEX. This material was supplied to us by Ten Cate. The fibre type is the carbon fibre T300J 3K and the weave pattern is a 5-harness satin weave with a mass per surface unit of 286 g/m^2. The 5-harness satin weave is a fabric with high strength in both directions and excellent bending properties.

The carbon PPS plates were hot pressed, only one stacking sequence was used for this study, namely $[(0^\circ,90^\circ)]_{4s}$ where $(0^\circ,90^\circ)$ represents one layer of fabric.

The in-plane elastic properties of the individual carbon PPS lamina were determined by the dynamic modulus identification method as described in [12] and are listed in Table 1.

The tensile strength properties were determined at the Technical University of Delft and are listed in Table 2.

The test coupons were sawn with a water-cooled diamond saw. The dimensions of the coupons are shown in Fig. 1 and the geometry of the end tabs was chosen according to the results from [13].

2.2. Equipment

All tensile tests were performed on a servo-hydraulic INSTRON 8801 tensile testing machine with a FastTrack 8800 digital controller and a load cell of ±100 kN. The quasi-static tests were displacement-controlled with a speed of 2 mm/min. For the alignment of the grips, the alignPro™ from INSTRON was used.

For the registration of the tensile data, a combination of a National Instruments DAQpad 6052E for fireWire, IEEE 1394 and the SCB-68 pin shielded connector were used.

Table 1
In-plane elastic properties of the individual carbon/PPS lamina (dynamic modulus identification method).

E_{11}	56.0	GPa
E_{22}	57.0	GPa
ν_{12}	0.033	–
G_{12}	4.175	GPa

Table 2
Tensile strength properties of the individual carbon/PPS lamina (Mechanical testing at TUDelft).

X_T	734.0	MPa
ε_{11}^{ult}	0.011	–
Y_T	754.0	MPa
ε_{22}^{ult}	0.013	–
S_T	110.0	MPa

The load, displacement and strain, given by the FastTrack controller, as well as the extra signals from strain gauges were sampled on the same time basis.

3. Experiments

3.1. Introduction

In part I of this study [1], the results of some of the quasi-static hysteresis tests have already been illustrated. However, all of the experiments discussed had one thing in common: all of them were hysteresis tests with increasing maximum load level. Before trying to find an explanation for the peculiar shape of the ν_{12}–ε_{xx} curve, first the behaviour of the material subjected to quasi-static cyclic loading with constant maximum load level needs to be examined. Indeed, for the hysteresis tests with increasing maximum load, an increase in permanent deformation and a decrease in Poisson's ratio were seen for each next loading cycle. However, it is unclear at which point new damage develops. Damage may grow from 0 MPa onwards during each loading, regardless of the loading history, or it could start growing at higher load levels, for instance the maximum load level of the previous loading cycle.

Since it was already confirmed in the first part of this study [1] that the transverse strain sensor used has no influence on the relationship between the Poisson's ratio and the longitudinal strain, the specimens considered here are instrumented with two strain gauges, as illustrated in Fig. 1.

Since the displacement speed did not seem to have a significant effect [1], all experiments were done at 2 mm/min. Various experiments were performed, again all yielding similar results, so only a few are shown here. Fig. 2 shows the stress–strain relationship of two of such tests. For both, again four cycles up to 100 MPa were done to assess the behaviour of the Poisson's ratio at low stress

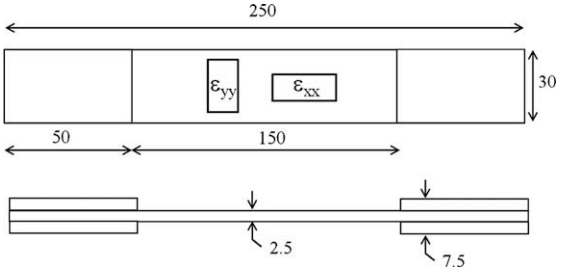

Fig. 1. Dimensions of the used tensile coupon, equipped with straight-end tabs of $[(0^\circ,90^\circ)]_{4s}$ carbon/PPS [13].

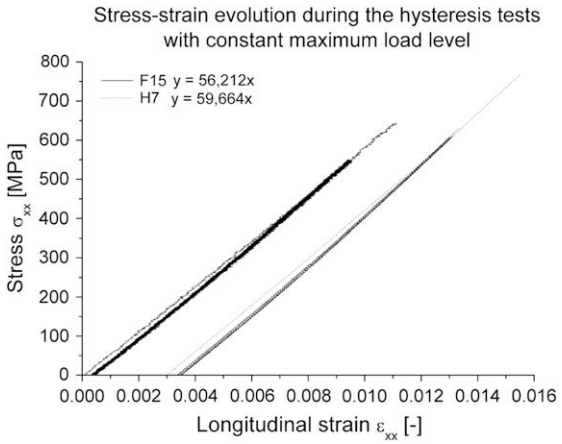

Fig. 2. Longitudinal stress as function of the longitudinal strain for the quasi-static hysteresis with constant load level.

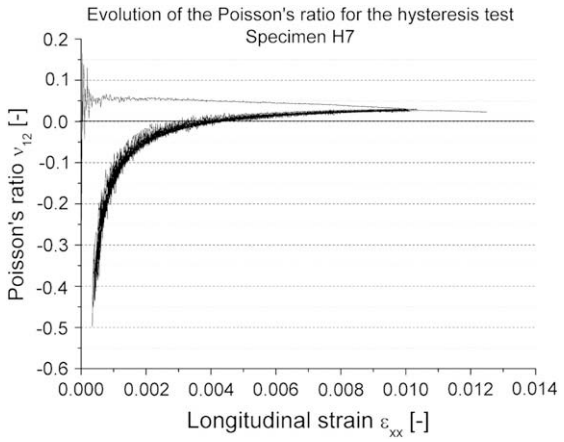

Fig. 4. The evolution of Poisson's ratio as function of the longitudinal strain.

levels, but similar results as in part I [1] were obtained, so these results are not shown here. Then, ten cycles were imposed on each specimen, after which the specimen was tested until failure. Specimen F15 endured ten cycles with a maximum load of 550 MPa and then failed at 640 MPa, and specimen H7 was tested at a maximum load of 600 MPa and, after that, it failed at 770 MPa. Both curves are given an offset in longitudinal strain of 0.003 for a clear image.

It should be noted that no stiffness degradation occurs and only limited permanent deformation is present. This permanent deformation is formed mainly during the first cycle. The evolution of the Poisson's ratio is shown in Fig. 3 for specimen F15 and in Fig. 4 for specimen H7.

The difference between these results and the results from the hysteresis tests with gradually increasing maximum load [1] cannot be missed. For the latter, a gradual increase in Poisson's ratio could clearly be seen, whereas here the curves for the different loading cycles overlap. This is even more the case for higher load levels (specimen H7). It appears that all changes to which the Poisson's ratio is sensitive, happen during the first loading, similar to the permanent deformation. Only a very slight decrease can be seen if the evolution of the Poisson's ratio is plotted against time. These evolutions are shown in Fig. 5 for specimen F15 and in Fig. 6 for specimen H7.

4. Discussion

From all experiments discussed both here and in part I of this study [1] it can be concluded that the carbon fabric-reinforced polyphenylene sulphide shows no stiffness degradation and only limited permanent deformation occurs. When cyclic loadings with increasing maximum stress are applied, the permanent deformation also increases with each load. However, when cyclic loadings with constant maximum stress are applied, the permanent deformation tends to form in the first loading cycles, and for the following cycles it only grows very little.

With respect to the Poisson's ratio, a decreasing Poisson's ratio is found. Similar to the permanent deformation, ν_{12} continuously decreases with increasing maximum load cycles and the different cycles can be clearly distinguished, but when the maximum load and the hysteresis remain

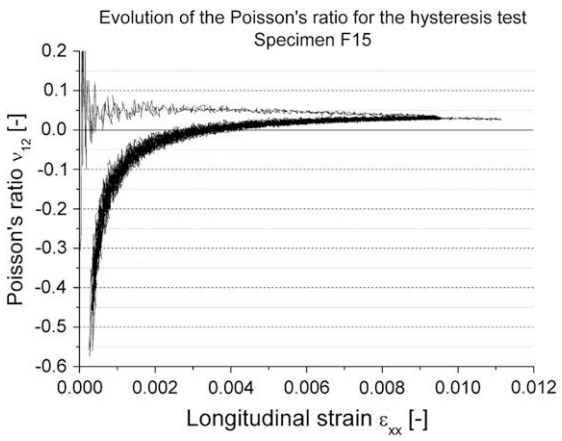

Fig. 3. The evolution of Poisson's ratio as function of the longitudinal strain.

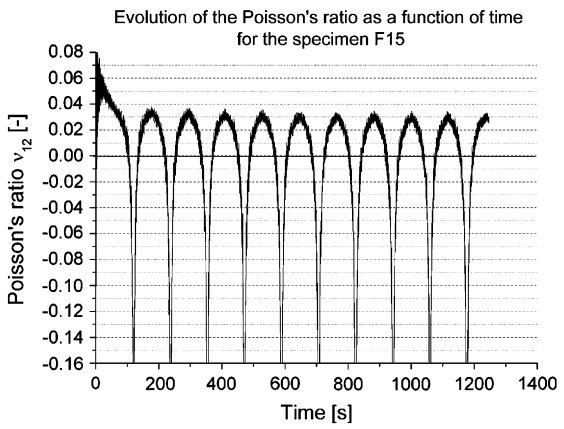

Fig. 5. The evolution of Poisson's ratio as function of time for the specimen F15.

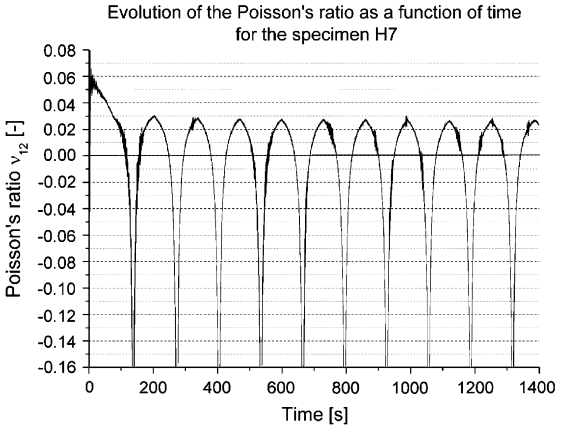

Fig. 6. The evolution of Poisson's ratio as function of time for the specimen H7.

constant, the ν_{12}–ε_{xx} curves almost coincide and very little decrease can be noted.

When the Poisson's ratio is plotted versus the longitudinal strain, a very peculiar evolution is found. From the different types of experiments conducted, it can be concluded that this behaviour is not caused by misalignment of the grips, nor by visco-elastic effects, since the shape of the curve remained the same for both 2 mm/min and 0.1 mm/min displacement speed. The effect is not caused by the strain gauge, since it also occurred when using optical fibre sensors. Both strain gauge and optical fibre are bonded to the surface, but the adhesive is not the driving force either, since the behaviour was also noted when using a (modified) transverse extensometer, for which no adhesive is necessary.

As such, it may be concluded that the typical shape from the curve is caused by the material itself.

In all curves, the Poisson's ratio was calculated by dividing the total strains:

$$\nu_{12}^{dam} = -\frac{\varepsilon_{22}^{total}}{\varepsilon_{11}^{total}} \tag{1}$$

It is well known that the total strain consists of an elastic strain and a permanent strain.

$$\nu_{12}^{dam} = -\frac{\varepsilon_{22}^{elas} + \varepsilon_{22}^{perm}}{\varepsilon_{11}^{elas} + \varepsilon_{11}^{perm}} \tag{2}$$

The definition of the Poisson's ratio in virgin state material is given in Equation (3), meaning that the ratio is found by dividing elastic strains:

$$\nu_{12}^{0} = \lim_{\varepsilon_{11}\to 0}\left(-\frac{\varepsilon_{22}}{\varepsilon_{11}}\right) \tag{3}$$

Considering this definition and the fact that the evolution of Poisson's ratio remained constant for the experiments with a constant low maximum stress of 100 MPa, it may be assumed that Equation (4) is valid:

$$\nu_{12}^{0} = -\frac{\varepsilon_{22}^{elas}}{\varepsilon_{11}^{elas}} \tag{4}$$

As such, Equation (2) can be rewritten as:

$$\nu_{12}^{dam} = -\frac{-\nu_{12}^{0}\varepsilon_{11}^{elas} + \varepsilon_{22}^{perm}}{\varepsilon_{11}^{elas} + \varepsilon_{11}^{perm}} \tag{5}$$

During the loading of the specimen, a permanent deformation will occur, as could be seen in the various experiments described, meaning that both ε_{11}^{perm} and ε_{22}^{perm} can be complicated functions of both stress and strain and the pre-loading history.

However, it is very unlikely that both permanent strains will decrease significantly during the unloading of a cycle, meaning they can be considered as constants, corresponding to a certain stress level. As such, Equation (5) can be considered as the following function during unloading:

$$\nu_{12}^{dam}(x) : x \to \frac{\nu_{12}^{0}x + \varepsilon_{22}^{perm,\sigma_{MAX}^{cycle}}}{x + \varepsilon_{11}^{perm,\sigma_{MAX}^{cycle}}} \tag{6}$$

This is no more than a hyperbolic function with a horizontal asymptote for y equal to ν_{12}^{0} and a vertical asymptote for x equal to $-\varepsilon_{11}^{perm,\sigma_{MAX}^{cycle}}$. As such, the typical behaviour is explained for the unloading part of the cyclic loading.

During the various experiments with constant maximum load level, it was noted that the permanent deformation had a significant increase for the first cycle, but for all the following cycles at the same load level the permanent deformation virtually did not grow. This might be explained as follows. By applying tension in one direction, the actual local tensile stresses of the matrix will be much higher than the applied stress, because of the residual compression of the fibres. As such damage (matrix cracks, de-bonding of the fibres) will occur once a certain global stress level is reached, allowing the compressed fibres to relax, causing permanent elongation, and form a new equilibrium in stresses and strains. Since the thermal stresses will not be uniformly distributed along the entire plate, because of non uniform cooling of the plate (some zones will cool faster than others), some fibres will be stressed more and are therefore allowed to relax sooner than other fibres.

The next loading cycle with the same stress level will only cause a very limited amount of damage, since at this maximum stress level there already was equilibrium. It is only for higher stress levels that new damage develops and a new equilibrium in stresses is formed.

Of course, a similar process will happen in the transverse direction. Due to damage of the matrix, the transverse fibres are allowed to relax the residual stresses, causing transverse elongation, which results in positive transverse strains.

A small comment can be made considering these thermal stresses and the preparation of the test samples. After sawing the specimens, some of the specimens tended to twist around their longitudinal axis; even some large plates had a slight saddle-like shape. Both phenomena prove that these residual stresses are indeed present.

Going back to the explanation on the Poisson's ratio, this means that Equation (6) is also valid for the loading of the next cycle until the stress level in this cycle is about the

same as the maximum stress from the previous cycle. From that point on, both ε_{11}^{perm} and ε_{22}^{perm} will continue to increase, which causes a different, slower evolution towards the horizontal asymptote, since ε_{11}^{perm} grows faster than ε_{22}^{perm} because the specimen is loaded along the warp direction. This and the fact that ν_{12}^{0} is smaller than one causes the denominator to increase more than the numerator, yielding a decreasing Poisson's ratio.

The vertical asymptote (for x equal to $-\varepsilon_{11}^{perm,\sigma_{MAX}^{cycle}}$) will shift to the left, which can also be seen in the experiments with increasing maximum load level. When the specimen is unloaded, the slope of the tangent in this point is steeper for the cycle with a lower maximum load level.

This is illustrated in Fig. 7, which is no more than a detailed image of one of the results depicted in Fig. 9 in the first paper [1], with tangent lines added. This effect is more visible for this experiment than for the others, since the difference in maximum load levels is 100 MPa, causing the curves to be further apart, and probably because of the lower testing speed, which seemed to decrease the noise on the signal.

At this point, no validated explanations for the occurrence of this permanent deformation can be given, only assumptions can be made. In order to determine whether this deformation is due to plastic deformation of the matrix, the occurrence of micro-cracks along or perpendicular to the fibres or other phenomena, a profound study of the micro-mechanical behaviour of this specific material is required.

The explanation given above can also be confirmed numerically. In Fig. 8, a theoretical evolution of the longitudinal and transverse strain is illustrated. An increasing permanent deformation was simulated both for the longitudinal and the transverse strain after each unloading. It should be noted that these values of the permanent deformation are chosen arbitrarily, just to illustrate the explanation above. This is not a model of the damage mechanics of the material under study.

The corresponding simulated evolution of the Poisson's ratio as a function of the longitudinal strain is shown in Fig. 9. It can be remarked that the typical hyperbolic shape is visible, validating the derivation above. Also, the effect of

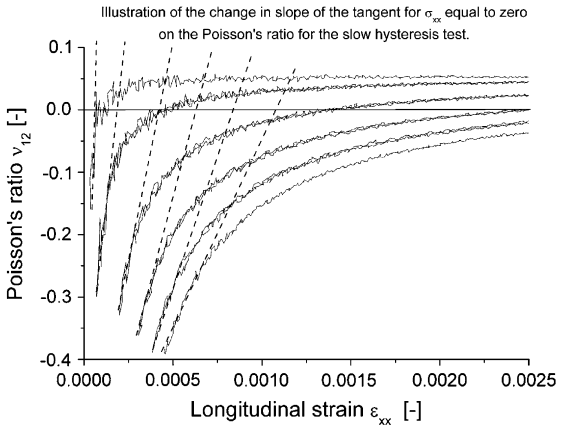

Fig. 7. Illustration of the decrease in slope of the tangent line for higher loading cycles.

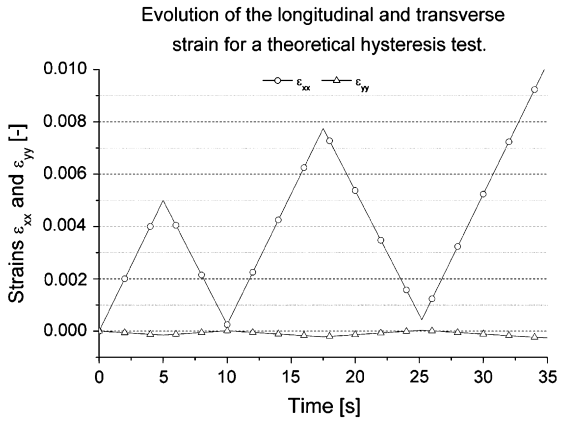

Fig. 8. Theoretical evolution of the ε_{xx} and ε_{yy}.

the permanent deformation after each loading cycle can be seen on the evolution towards the horizontal asymptote. For this theoretical case, the horizontal asymptote occurs for $y = 0.03$ and each loading evolves slower towards this asymptote than the previous one, creating the decrease in the Poisson's ratio at maximum load of each loading cycle.

Finally, this explanation can also be verified experimentally. Indeed, by recalibrating the strain sensors after each loading and unloading, the permanent deformation only has limited influence, since it cannot accumulate throughout the experiment, it only grows during the loading part of each cycle. As such, a limited hyperbolic behaviour is expected during the unloading, but if the deduction above is correct, it should be a lot less dominant on the general view of the graph.

For this validation, two types of experiments were performed. For the first, a hysteresis test with increasing maximum load was done, similar to the experiments in the first part of this study, meaning the first loading was up to 100 MPa and for each next loading, the maximum stress level was increased by 50 MPa. The evolution of both the longitudinal and transverse strain is illustrated in Fig. 10. Although it is very hard to see, due to the scale, after each unloading a very small amount of permanent deformation is present, for both strains. Balancing the sensors assures that the next loading cycle starts again at a zero strain level.

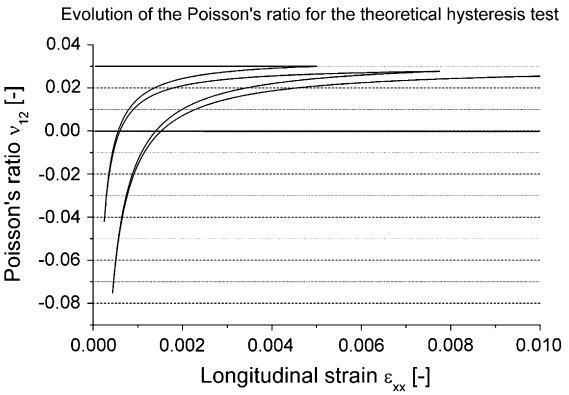

Fig. 9. Theoretical evolution of ν_{12} as function of ε_{xx}.

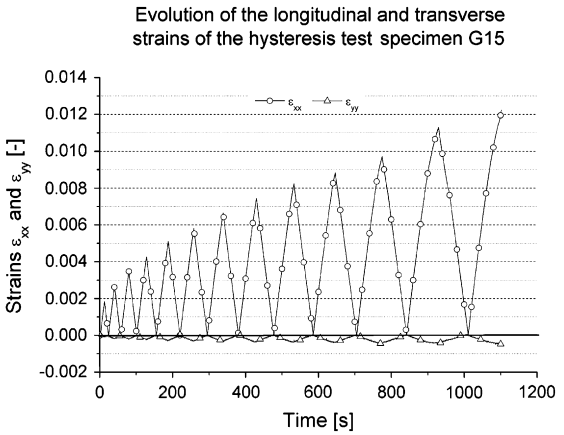

Fig. 10. Evolution of ε_{xx} and ε_{yy} as a function of time for the 'balanced' hysteresis test on G15.

Fig. 11 shows the corresponding evolution of Poisson's ratio as a function of the longitudinal strain. It can clearly be seen that the hyperbolic nature is very limited and it should be noted that it only occurs for the unloading part of the curve.

For the second type of experiment, a hysteresis test with constant maximum load is considered. If the theoretical explanation is correct, then balancing the strain sensors after each loading cycle would result in only one hyperbolical curve, namely the one after the first loading. Similar to specimen H7, a maximum load of 600 MPa was chosen, but only 10 loading cycles were performed, the specimen was not loaded till failure. Fig. 12 shows the evolution of the Poisson's ratio for this experiment and, as expected, only the first loading cycle (grey, dotted curve) is hyperbolic, all other curves are fairly constant, with exception of course for the scatter for lower strain levels.

As such, it is also verified experimentally that the theoretical deduction above is valid and the hyperbolical nature of the ν_{12}–ε_{xx} curve can be ascribed to the occurrence of permanent deformation.

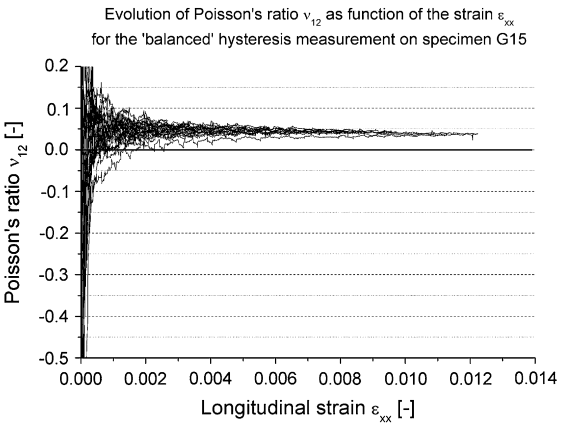

Fig. 11. The evolution of Poisson's ratio as function of the longitudinal strain for the 'balanced' hysteresis test on G15.

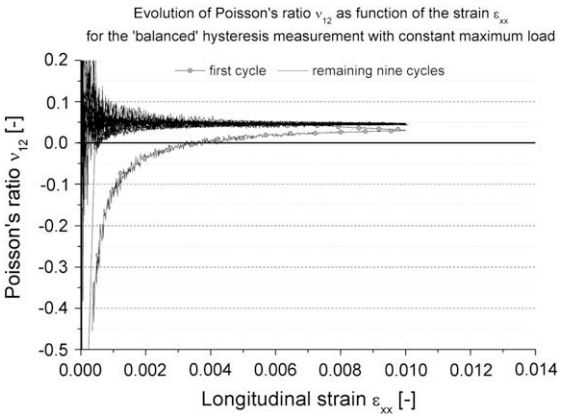

Fig. 12. The evolution of Poisson's ratio as function of the longitudinal strain for the 'balanced' hysteresis test with constant maximum load level.

5. Conclusions

This paper investigated the origin of the hyperbolic nature of the relation between the Poisson's ratio and the longitudinal strain. Based on the results of the previous paper and those presented here, an analytical explanation, based on permanent deformation, is given to explain the hyperbolic nature of the ν_{12}–ε_{xx} curve. This deduction was then validated both theoretically and experimentally. The latter was done by performing extra hysteresis tests during which, after each unloading, the strain sensors were recalibrated, therefore eliminating the influence of accumulating permanent deformation.

This analytical model and the obtained insights are very important for the Poisson's ratio to be considered as a reliable damage parameter or sensor.

Also, based on the hysteresis tests with constant maximum load, it can again be concluded that the carbon fabric-reinforced PPS shows no stiffness degradation and only limited permanent deformation. The latter only occurs during the first loading cycle and for the following cycles, virtually no growth can be noticed.

Acknowledgements

The authors are highly indebted to the university research fund BOF (Bijzonder Onderzoeksfonds UGent) for sponsoring this research and to Ten Cate Advanced Composites for supplying the material. They would also like to thank Luc Van den Broecke, for his assistance in the laboratory and Chris Bonne, for his help with the strain gauge measurements.

References

[1] I. De Baere, W. Van Paepegem, J. Degrieck, On the nonlinear evolution of the Poisson's ratio under quasi-static loading for a carbon fabric-reinforced thermoplastic, Part I: influence of the sensor 28 (2) (2009) 196–203.
[2] F. Gao, L. Boniface, S.L. Ogin, P.A. Smith, R.P. Greaves, Damage accumulation in woven-fabric CFRP laminates under tensile loading: part 1. Observations of damage accumulation, Composites Science and Technology 59 (1) (1999) 123–136.
[3] M. Surgeon, E. Vanswijgenhoven, M. Wevers, O. Van der Biest, Transverse cracking and Poisson's ratio reduction in cross-ply

carbon fibre-reinforced polymers, Journal of Materials Science 34 (22) (1999) 5513–5517.
[4] F. Gao, L. Boniface, S.L. Ogin, P.A. Smith, R.P. Greaves, Damage accumulation in woven-fabric CFRP laminates under tensile loading: 2. Modelling the effect of damage on macro-mechanical properties, Composites Science and Technology 59 (1) (1999) 137–145.
[5] P.A. Smith, J.R. Wood, Poisson ratio as a damage parameter in the static tensile loading of simple crossply laminates, Composites Science and Technology 38 (1) (1990) 85–93.
[6] P.P. Parlevliet, H.E.N. Bersee, A. Beukers, Residual stresses in thermoplastic composites – a study of the literature. Part III: effects of thermal residual stresses, Composites Part A: Applied Science and Manufacturing 38 (6) (2007) 1581–1596.
[7] L. DiLandro, M. Pegoraro, Evaluation of residual stresses and adhesion in polymer composites, Composites Part A: Applied Science and Manufacturing 27 (9) (1996) 847–853.
[8] F. Bassa, L. Boniface, K. Jones, S.L. Ogin, On the behaviour of the residual strain produced by matrix cracking in cross-ply laminates, Composites Part A 29 (1998) 1425–1432.
[9] P.P. Parlevliet, H.E.N. Bersee, A. Beukers, Residual stresses in thermoplastic composites—a study of the literature—part I: formation of residual stresses, Composites Part A: Applied Science and Manufacturing 37 (11) (2006) 1847–1857.
[10] M. Senel, H. Akbulut, M. Toparli, Residual stress analysis in symmetric thermoplastic laminated plates under thermal loads: analytic solution, Journal of Thermoplastic Composite Materials 17 (6) (2004) 481–507.
[11] C. Filiou, C. Galiotis, In situ monitoring of the fibre strain distribution in carbon-fibre thermoplastic composites 1. Application of a tensile stress field, Composites Science and Technology 59 (14) (1999) 2149–2161.
[12] I. De Baere, W. Van Paepegem, J. Degrieck, H. Sol, D. Van Hemelrijck, A. Petreli, Comparison of different identification techniques for measurement of quasi-zero Poisson's ratio of fabric reinforced laminates, Composites Part A 38 (9) (2007) 2047–2054.
[13] I. De Baere, G. Luyckx, E. Voet, W. Van Paepegem, J. Degrieck, On the feasibility of optical fibre sensors for strain monitoring in thermoplastic composites under fatigue loading conditions, Special Issue of Optics and Lasers in Engineering 47 (2009) 403–411.